



Enhanced catalytic performance of zeolite ZSM-5 for conversion of methanol to dimethyl ether by combining alkaline treatment and partial activation



Ying Wei^a, Petra E. de Jongh^a, Matteo L.M. Bonati^b, David J. Law^b, Glenn J. Sunley^b, Krijn P. de Jong^{a,*}

^a *Inorganic Chemistry and Catalysis, Debye Institute for Nanomaterials Science, Utrecht University, Universiteitsweg 99, 3584 CG Utrecht, Netherlands*

^b *BP International Limited, Conversion Technology Centre, Hull Research and Technology Centre, Kingston Upon Hull HU12 8DS, United Kingdom*

ARTICLE INFO

Article history:

Received 15 September 2014

Received in revised form

11 December 2014

Accepted 14 December 2014

Available online 22 December 2014

Keywords:

Methanol dehydration

Dimethyl ether

Zeolite ZSM-5

Alkaline treatment

Partial activation

ABSTRACT

Zeolite ZSM-5 (MFI) due to its excellent hydrothermal stability and high catalytic activity for methanol dehydration to dimethyl ether (MTD) has been considered for use in combination with a methanol synthesis catalyst, such as Cu/ZnO/Al₂O₃, in the conversion of syngas to dimethyl ether. However, the decline of dimethyl ether selectivity and catalytic activity over ZSM-5 by the formation of hydrocarbons and coke at optimum operation temperature of Cu/ZnO/Al₂O₃ catalyst impedes industrial application. In this work, for the first time the effects of alkaline treatment combined with partial activation on the catalytic performance of ZSM-5 catalysts with different Si/Al ratio have been studied for MTD reaction. The relationship between the physicochemical properties and catalytic performance has been assessed from the combined results of XRD, SEM, N₂ physisorption, NH₃-TPD, elemental analysis, online-GC and other characterization techniques. The results show that at a reaction temperature of 300 °C and WHSV of 13 g g⁻¹ h⁻¹, all the parent and alkaline-treated ZSM-5 after full activation at 500 °C exhibited a decline of dimethyl ether selectivity and methanol conversion over time. Alkaline treatment improved DME selectivity over ZSM-5 with an Si/Al ratio of 25, which could be ascribed to the formation of extra mesoporosity enhancing the diffusion capability and decreasing the probability of secondary reactions of DME to hydrocarbons. A decrease of the activation temperature led to a significantly improved DME selectivity for all parent and alkaline-treated ZSM-5 because ammonium cations were selectively retained in the structure and blocked the strong acid sites that brought about side-reactions. ZSM-5 with Si/Al ratio of 25 modified by combining alkaline treatment and partial activation, due to the synergy effect of moderated acidity and enhanced diffusion capability, exhibited improved catalytic performance with almost 100% DME selectivity, near 84% methanol conversion and excellent stability during 4 days of reaction.

© 2014 Elsevier B.V. All rights reserved.

1. Introduction

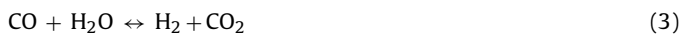
Dimethyl ether (DME) is an important chemical with traditional applications such as aerosol propellant, refrigerant and intermediate for the production of dimethyl sulfate. In recent years, with increasingly stringent environmental regulations and high crude oil prices, DME has been considered as an alternative fuel because it can be produced from non-petroleum feedstocks and meanwhile exhibits clean features such as low emission of NO_x, SO_x, particulate matter and combustion noise. The emerging applications include LPG substitute for home cooking and heating, gas turbine

fuel for power generation, alternative diesel fuel for transportation of vehicles with pressure-ignition engines etc. [1–4]. In view of the growing demand, more attention is paid to the synthesis of DME by both industrial and academic communities.

There are currently two main processes to produce DME in industry. One is a two-step synthesis process including the syngas to methanol process over Cu/ZnO/Al₂O₃ catalyst followed by the methanol dehydration to DME (MTD) process over a solid acid catalyst [5]. The alternative is a one-step synthesis process directly from syngas to DME (STD), over a hybrid catalyst comprising a methanol-synthesis catalyst and a solid acid catalyst for methanol dehydration [6]. The STD reactions are supposed to be composed of methanol synthesis (1), methanol dehydration (2) and water gas shift (3) reactions, with the overall reaction (4) as shown below. Compared with the two-step process, one-step STD process allows

* Corresponding author. Tel.: +31 30 2536762; fax: +31 30 2511027.
E-mail address: k.p.dejong@uu.nl (K.P. de Jong).

a simple reactor design with low DME product cost and favors the kinetics of the methanol synthesis, in particular for CO-rich synthesis gas from coal or biomass, giving rise to high CO equilibrium conversion and less demand on hydrogen [4,7].



Various solid acid catalysts such as $\gamma\text{-Al}_2\text{O}_3$ [5,8–13], niobia-modified alumina [14], $\text{TiO}_2\text{-ZrO}_2$ [15], sulfated zirconia [16], mesoporous silicates [17,18], zeolites [5,10,19–27] and zeotypes [28–30] have been studied for methanol dehydration. Among these catalysts, $\gamma\text{-Al}_2\text{O}_3$ is a very attractive and intensely investigated candidate since it is cost-effective and exhibits excellent thermal and mechanical stability, large surface area and high selectivity toward DME. Compared with $\gamma\text{-Al}_2\text{O}_3$, zeolites are considered as an even better choice due to their higher catalytic activity at low reaction temperature and much better stability in the presence of water, a product of this reaction. However, for a one-step process, undesirable by-products such as hydrocarbons and even coke are likely to form on zeolites at an optimum temperature of about 260 °C for the methanol synthesis catalyst $\text{Cu/ZnO/Al}_2\text{O}_3$, which will thus lower the DME selectivity and deactivate the catalyst [4,7,31]. Many studies have been carried out to understand the factors influencing the catalytic performance of different zeolites in the methanol to hydrocarbon (MTH) reactions [7,32–34]. It has been found that the conversion and selectivity of MTH are dependent on the strength and the density of the acid sites, as well as the pore structure of zeolite.

ZSM-5 is a most studied or used zeolite for methanol conversion and other important catalytic processes in chemistry industry, due to its unique framework topology, very high hydrothermal stability and easily modified physicochemical properties such as acidity and texture [32,33,35,36]. ZSM-5 framework contains two intersecting channel systems, with one straight channel parallel to [010] and the other sinusoidal running parallel to [001] defined by 10-membered ring openings of $5.3 \text{ \AA} \times 5.6 \text{ \AA}$ and $5.1 \text{ \AA} \times 5.5 \text{ \AA}$, respectively. The typical products of methanol conversion over ZSM-5 include olefins, aromatics and paraffins in addition to DME, because the channels are wide enough even for tetramethylbenzene to diffuse and the intersections of the channels provide enough volume for cyclization reactions and intermolecular hydride transfer reactions [32,33].

To achieve improved performance for DME synthesis, research has been focused on moderating the acidity of ZSM-5 because the strong acid sites on ZSM-5 have been regarded as active sites for the side-reactions and the main reason for the catalyst deactivation. The methods include deactivating ZSM-5 with ammonia or alkyl amine followed with reactivation by thermal treatment [31], and modifying ZSM-5 with Na, Mg, Al, Zr or Zn oxides by wet impregnation with metal salts solution [37–40]. These methods remarkably improved DME selectivity and catalyst stability due to the removal of strong acid sites. On the other hand, work has been carried out to alleviate diffusion limitation imposed by the small micropores of ZSM-5 structure and consequently avoid the occurrence of secondary reaction and the formation of coke. For example, Rownaghi et al. [41] investigated the MTD reaction on ZSM-5 nanocrystals and found that methanol conversion and DME selectivity could be enhanced by decreasing crystal size. Tang and Li et al. [42,43] showed that ZSM-5/MCM-41 composite molecular sieves could give good activity and selectivity over a large temperature range. Yang et al. [44] synthesized hierarchical mesoporous ZSM-5 zeolites by using small organic cations and mesosized cationic

polymers and found it exhibited better stability than conventional microporous ZSM-5. Based on these achievements, it could be expected that a tailored ZSM-5 zeolite which combines moderate acidity and enhanced diffusion capability would offer a significantly optimized catalyst for STD process operating under commercially relevant condition.

Alkaline treatment is a post-synthesis modification process that creates hierarchical zeolites by desilication, i.e. leaching silicon from the framework. Although a wide range of approaches including synthesizing nano-zeolites, zeolites with mesopore template and zeolite composites have been developed in achieving hierarchical structure, alkaline treatment has been thought of as a promising method for industrial-scale implementation especially when health–safety–environment issues and production costs are taken into account [45–47]. Mesoporous zeolites obtained by desilication have shown improved performance in various catalysis reactions. For instance, Svelle and Ryoo et al. reported that alkaline-treated ZSM-5 showed longer catalyst lifetime with increased resistance toward coking than conventional ZSM-5 for the methanol-to-hydrocarbons (MTH) reaction due to the improved diffusivity [48,49].

Zeolite catalysts are generally synthesized in the presence of Na^+ cations sometimes together with organic templates. Na^+ -form zeolite is usually obtained after the removal of organics by calcination, then ion-exchanged to NH_4^+ -form, and finally activated to H^+ -form by a thermal treatment at about 500 °C prior to catalysis. It has been reported that the cation has an obvious influence on the catalytic performance of ZSM-5 in the liquid-phase dehydration of methanol to DME [37]. NH_4^+ and H^+ -form were much more active than Na^+ -form, while the NH_4^+ -form exhibited higher methanol conversion and DME selectivity than that of H^+ -form. These findings were explained by the difference of their acidity with the order of H^+ -form > NH_4^+ -form > Na^+ -form.

In this work, we have investigated the effect of alkaline treatment and activation temperature on commercial NH_4^+ -form ZSM-5 zeolites with different Si/Al ratio for the MTD reaction. The relationship between catalytic performance and catalyst physicochemical properties such as acidity and texture properties was discussed based on the results of X-ray diffraction (XRD), scanning electron microscope (SEM), N_2 physisorption, CHN elemental analysis, inductively coupled plasma (ICP), ammonia-temperature programmed desorption (NH_3 -TPD), thermogravimetric analysis (TGA), nuclear magnetic resonance (NMR) and gas chromatography (GC). We found that the ZSM-5 catalyst modified by the combination of alkaline treatment and partial activation showed enhanced catalytic performance due to its moderated acidity and improved diffusion capability.

2. Experimental

2.1. Catalyst preparation

The parent ZSM-5 zeolites in NH_4^+ -form were purchased from Zeolyst company including CBV2314 (Si/Al = 12 at/at), CBV524G (Si/Al = 25 at/at) and CBV8014 (Si/Al = 40 at/at), which were designated as ZSM-5(*n*), *n* represents Si/Al atomic ratio. Alkaline treatment was performed at a fixed condition according to the literature [46], in which 0.5 g parent zeolite was added to 30 ml preheated 0.2 M NaOH solution (p.a., Merck) at 65 °C with stirring for 30 min. This was followed by filtration with demineralized water until the pH of filtrate was 7 and drying at 120 °C overnight. Subsequently, ion-exchange was performed in an aqueous 1 M NH_4NO_3 (p.a., Acros) solution at 80 °C for 24 h, followed by filtration and washing with demineralized water. Per gram of zeolite, 100 ml NH_4NO_3 solution was used. This procedure was repeated three

times to ensure complete removal of sodium ions. The obtained samples were named as ZSM-5(*n*)-AT, AT represents alkaline treatment.

2.2. Catalytic testing

The catalytic testing was performed in a fixed-bed quartz reactor (4 mm i.d.). 40 mg ammonium form of parent and alkaline-treated ZSM-5 catalyst particles (212–425 μm) were loaded and in situ activated in a flow of 33 ml/min N₂ at 300, 350, 400 or 500 °C for 2 h. Methanol (≥99.9%, Sigma–Aldrich) was fed with a flow of 0.011 ml/min using an HPLC pump and evaporated at 177 °C through 33 ml/min carrier gas N₂. The weight hourly space velocity (WHSV) was 13 g of methanol per gram catalyst per hour (g g⁻¹ h⁻¹), if not otherwise mentioned. The reaction was carried out at 160 or 300 °C and atmospheric pressure. The reaction products were analyzed using an on-line gas chromatography (Varian Bruker 450-GC) equipped with a capillary column (PoraPLOT-U) and flame ionization detector (FID). Methanol conversion (*X*_{methanol}), DME selectivity (*S*_{DME}) and ethylene selectivity (*S*_{ethylene}) were defined as:

$$X_{\text{methanol}} = \frac{F_{\text{methanol, in}} - F_{\text{methanol, out}}}{F_{\text{methanol, in}}} \times 100\%$$

$$S_{\text{DME}} = \frac{2F_{\text{DME, out}}}{F_{\text{methanol, in}} - F_{\text{methanol, out}}} \times 100\%$$

$$S_{\text{ethylene}} = \frac{2F_{\text{ethylene, out}}}{F_{\text{methanol, in}} - F_{\text{methanol, out}}} \times 100\%$$

where *F*_{methanol, in}, *F*_{methanol, out}, *F*_{DME, out} and *F*_{ethylene, out} are the molar flows of methanol at inlet, outlet and the molar flows of DME and ethylene at outlet, respectively.

2.3. Catalyst characterization

Powder X-ray diffraction (XRD) patterns were obtained using a Bruker-Axs D8 series 2 with a Co Kα_{1,2} source (λ = 0.179 nm). Morphology was determined with a Tecnai FEI XL 30SFEG SEM at 15 kV. The porosity of the samples was studied using N₂ physisorption isothermal, which were recorded with a Micromeritics Tristar 3000 at –196 °C. Prior to the physisorption measurements, the samples were dried overnight at 300 °C in flowing nitrogen. The *t*-plot method [50] was applied to obtain the micropore volume and the external surface area. Pore size distributions were obtained from the adsorption branch using the BJH-method [51]. NH₃-TPD was performed with a Micromeritics Autochem II. About 100 mg of sample was dried with a heating ramp of 10 °C min⁻¹ to 600 °C and kept there for 60 min after which the sample was cooled down to 100 °C. After saturating the sample with ammonia, a 60 min dwell time was applied to obtain a stable baseline. Subsequently the temperature was increased to 600 °C with a heating rate of 5 °C min⁻¹. ²⁷Al MAS NMR experiments were performed at room temperature on a Varian VNMRs spectrometer using a 4 mm probe. The ²⁷Al chemical shift was referenced to 1 M Al(NO₃)₃ in H₂O. TGA experiments were carried out on a Perkin Elmer Pyris 1 TGA from room temperature to 800 °C with a heating rate of 5 °C min⁻¹ under a flow of argon and oxygen. The Al and Si contents of these catalysts were determined by inductively coupled plasma (ICP) analysis using a Philips PU 7000 ICP-AES-spectrometer. The CHN elemental analysis was conducted on an Exeter Analytical CE440 elemental analyser.

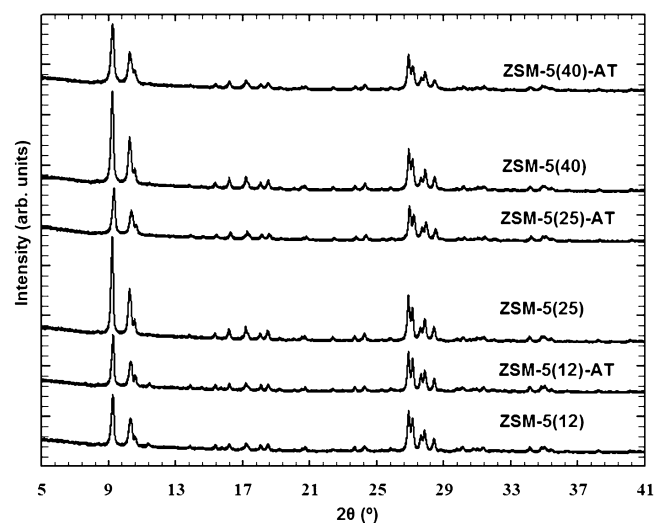


Fig. 1. Powder X-ray diffraction patterns of parent and alkaline-treated ZSM-5 catalysts.

3. Results and discussion

3.1. Physicochemical properties

Fig. 1 shows the powder X-ray diffraction patterns of parent and alkaline-treated ZSM-5 catalysts with different Si/Al ratio. These results demonstrate that during the alkaline treatment the crystal structure of these catalysts was well preserved and no new phase was formed. Moreover, we observed that after alkaline treatment the crystallinity of ZSM-5(25)-AT and ZSM-5(40)-AT distinctly decreased according to the intensity of the diffraction peak at $2\theta = 9.24^\circ$, while ZSM-5(12)-AT exhibited similar crystallinity to that of the parent zeolite. It indicates that ZSM-5(25) and ZSM-5(40) suffered more severe leaching of the framework atoms than ZSM-5(12) during the treatment in NaOH solution.

SEM images presented in Fig. 2 show that both ZSM-5(12) and ZSM-5(25) contained cubic-like crystallites of 0.5–1.0 μm in size agglomerated into large particles, while ZSM-5(40) consisted of agglomerated small grain-like crystallites of ~50 nm in size. After alkaline treatment, ZSM-5(12)-AT showed well preserved morphology and aggregation with high mass yield of 86%, while ZSM-5(25)-AT and ZSM-5(40)-AT exhibited more irregular morphology and less compact aggregation with relative lower yield of 53% and 57%, respectively, which could be ascribed to the occurrence of desilication reaction during the alkaline treatment. These observations are in good agreement with the XRD analysis results.

Fig. 3 shows the N₂ physisorption isotherms and BJH pore size distributions of the parent and alkaline-treated ZSM-5 catalysts. The textural parameters of these catalysts are summarized in Table 1. All parent samples displayed similar isotherms with high uptakes of N₂ at low partial pressure and a small hysteresis loop

Table 1
Textural property of parent and alkaline-treated ZSM-5 catalysts.

Samples	<i>A</i> _{BET} (m ² g ⁻¹)	<i>A</i> _{ext} (m ² g ⁻¹)	<i>V</i> _{micro} (cm ³ g ⁻¹)	<i>V</i> _{total} (cm ³ g ⁻¹)
ZSM-5(12)	372	16	0.10	0.21
ZSM-5(12)-AT	361	29	0.11	0.23
ZSM-5(25)	409	34	0.10	0.27
ZSM-5(25)-AT	432	115	0.09	0.56
ZSM-5(40)	420	41	0.11	0.27
ZSM-5(40)-AT	429	80	0.09	0.57

Here the value is italicised bold in order to facilitate the reading when comparison between the parents or between alkaline-treated samples are needed.

* *P*/*P*₀ = 0.995.

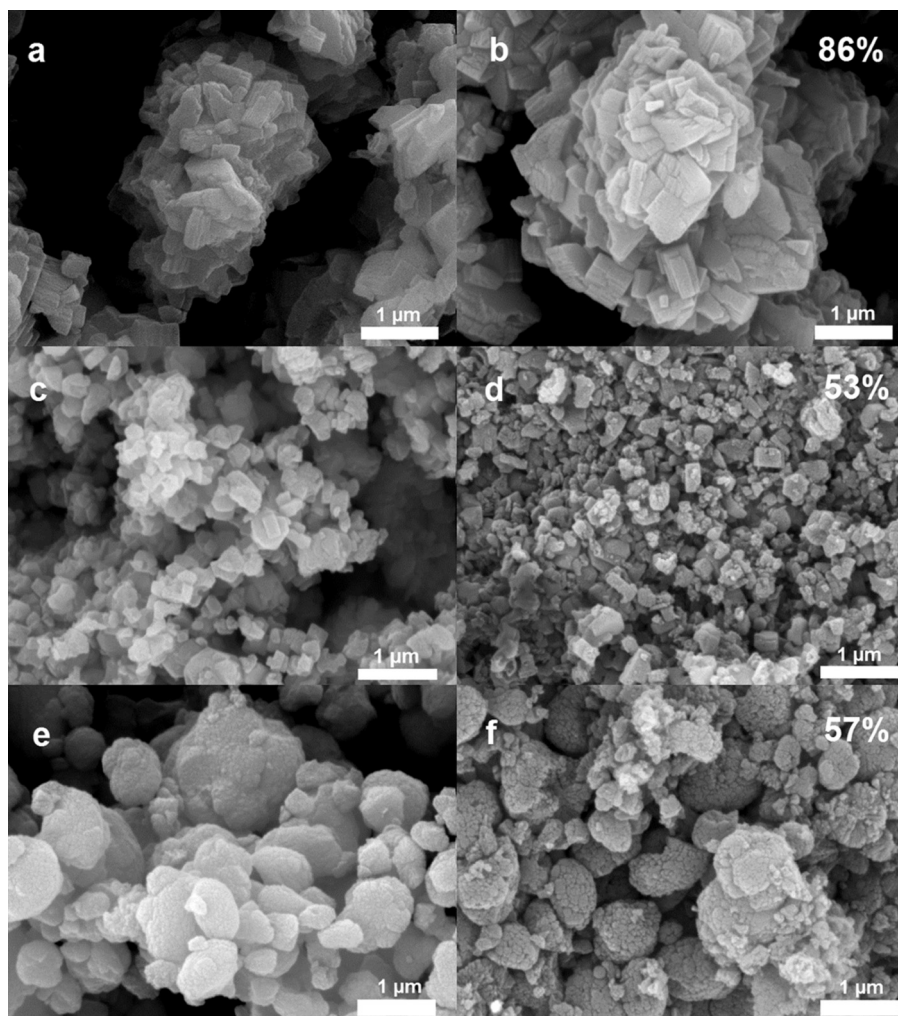


Fig. 2. SEM images of parent and alkaline-treated ZSM-5 catalysts with the yield (wt%) inset: (a) ZSM-5(12), (b) ZSM-5(12)-AT, (c) ZSM-5(25), (d) ZSM-5(25)-AT, (e) ZSM-5(40) and (f) ZSM-5(40)-AT.

at P/P_0 between 0.5 and 0.9. These results indicate that the parent ZSM-5 have high microporosity and also a little inter-crystal mesoporosity possibly related to the aggregation of the crystals. After alkaline treatment, isotherm and BJH pore size distribution of ZSM-5(12)-AT were similar to that of ZSM-5(12). The external surface area increased from 16 to 29 m² g⁻¹, while the total pore volume showed little change. It indicates that there was very limited extra porosity formed, which was due to the Si/Al ratio being well below the range of 25–50 that is reported to be necessary to introduce mesoporosity [52]. The isotherms of ZSM-5(25)-AT and ZSM-5(40)-AT as compared with that of the parent materials exhibited a similar uptake of N₂ at low pressure and a distinctly enhanced uptake of N₂ at higher pressure with a hysteresis loop. The BJH pore size distribution curves exhibited pores ranging from 3 nm to 250 nm. The external surface area, sometimes referred to the mesoporous surface area, increased from 34 to 115 m² g⁻¹ and 41 to 80 m² g⁻¹, the total pore volume increased from 0.27 to 0.56 cm³ g⁻¹ and 0.27 to 0.57 cm³ g⁻¹, while the micropore volume slightly decreased from 0.10 to 0.09 cm³ g⁻¹ and 0.11 to 0.09 cm³ g⁻¹, respectively. These results indicate that the alkaline treatment created extra mesoporosity and macroporosity over ZSM-5(25) and ZSM-5(40) without obvious loss of the microporosity.

NH₃-TPD measurements were carried out to characterize the acidity of these catalysts. As shown in Fig. 4, the ammonia desorption curves were typically divided into two peaks in the range of

100–250 and 250–550 °C representing the weak and strong acid sites of HZSM-5, respectively [38]. The acid site amounts have been quantified as shown in Table 2. For parent ZSM-5, both total and strong acid site amount decreased with increasing Si/Al ratio in the order of ZSM-5(12) > ZSM-5(25) > ZSM-5(40). Upon alkaline treatment, the strong acid site amount of ZSM-5(12)-AT and ZSM-5(25)-AT had a slight increase, while that of ZSM-5(40)-AT had a distinct increase compared with the parent zeolites. The increase

Table 2

The acid sites density and Si/Al ratio of the parent and alkaline-treated ZSM-5 catalysts.

Samples	Acid sites density (mmol g ⁻¹)			Si/Al atomic ratio ^b
	Weak ^a	Strong ^a	Total ^a	
ZSM-5(12)	0.04	0.80	0.82	11.9
ZSM-5(12)-AT	0.03	0.82	0.85	11.3
ZSM-5(25)	0.29	0.31	0.60	26.4
ZSM-5(25)-AT	0.33	0.33	0.66	15.8
ZSM-5(40)	0.21	0.25	0.46	39.8
ZSM-5(40)-AT	0.32	0.34	0.66	23.9

Here the value is italicised bold in order to facilitate the reading when comparison between the parents or between alkaline-treated samples are needed.

^a Determined by NH₃-TPD.

^b Determined by ICP analysis.

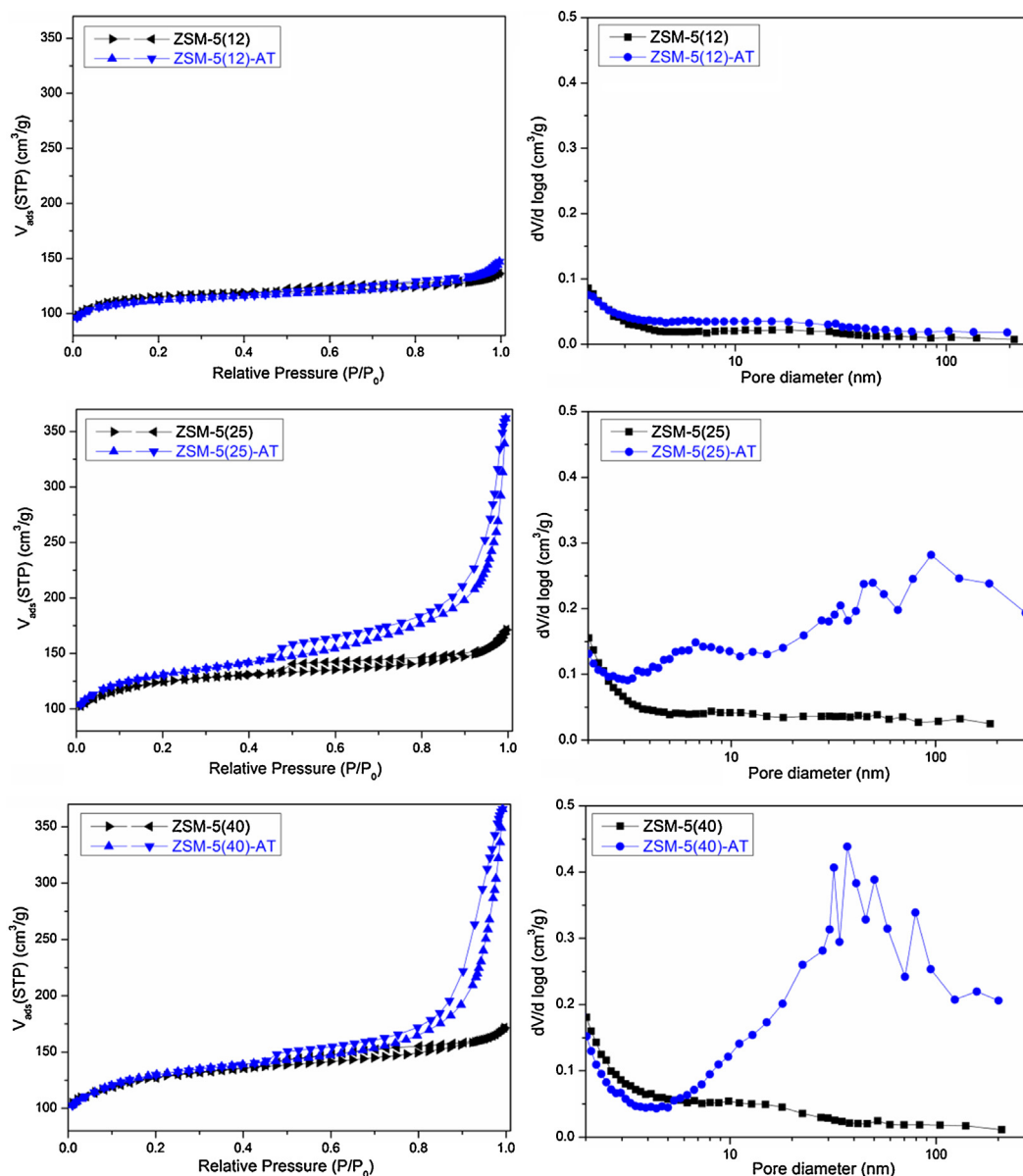


Fig. 3. Nitrogen physisorption isotherms (left) and BJH pore size distribution curves derived from the adsorption branch of isotherms (right) of parent and alkaline-treated ZSM-5 catalysts.

of acid density over ZSM-5(40)-AT could be due to the increase of the framework Al content caused by the preferential extraction of framework silicon over aluminum during the alkaline treatment [53], which is supported by the decreased Si/Al atomic ratio according to the ICP analysis results listed in Table 2. Noteworthy, the acid strength of strong acid sites over ZSM-5(12)-AT decreased as compared with that of ZSM-5(12), which was indicated by the position of ammonia desorption peaks center that decreased from 405 to 395 °C after the alkaline treatment.

4. Catalytic performance

Catalytic performance of parent and alkaline-treated ZSM-5 catalysts for methanol dehydration was investigated after full activation at 500 °C and at reaction temperatures of 160 and 300 °C, respectively. At 160 °C, all these catalysts showed stable methanol conversion within 4 h of reaction time. As shown in Fig. 5, the methanol conversion decreased with increasing of Si/Al ratio in the sequence of ZSM-5(12) > ZSM-5(25) > ZSM-5(40). The

alkaline-treated ZSM-5 exhibited a slight increase of catalytic activity as compared with that of parent zeolites, which can be ascribed to the increase of acid site density as evidenced by NH₃-TPD. Moreover, methanol conversion shows a dependence on strong acid site density in contrast to total acid site density (Fig. 6). This result suggests that weak acid sites are inactive for methanol dehydration at this temperature. As shown in Fig. 5, at 300 °C, all the catalysts displayed higher catalytic activity with similar methanol conversion of about 84% close to the equilibrium conversion [54]. The methanol conversion had a slight decay concomitant with the color of catalyst turning dark with increasing the reaction time, which indicates the occurrence of catalyst deactivation.

At 160 °C, it was found that DME selectivity over all these catalysts was 100% and no by-products were found in the effluent. However, the DME selectivity dropped below 100% at 300 °C with the appearance of hydrocarbons such as light olefins in the effluent as shown in Fig. 7. The parent zeolites, ZSM-5(40)/ZSM-5(25) had high/medium initial DME selectivity decreasing with time on stream (TOS), while ZSM-5(12) had low initial DME selectivity

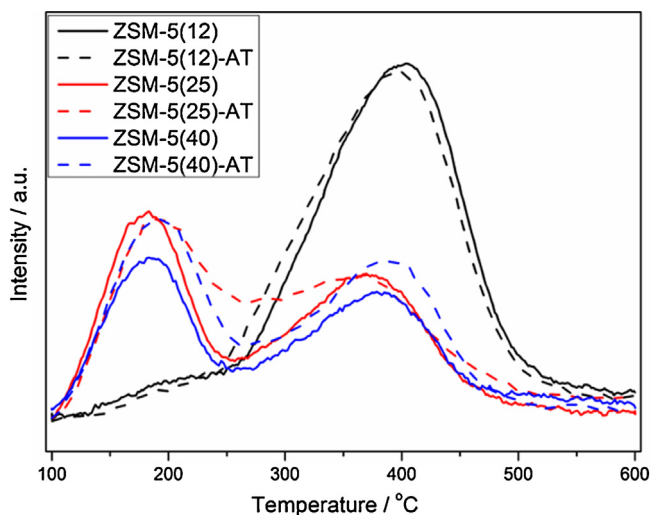


Fig. 4. NH_3 -TPD desorption profiles of parent and alkaline-treated ZSM-5 catalysts.

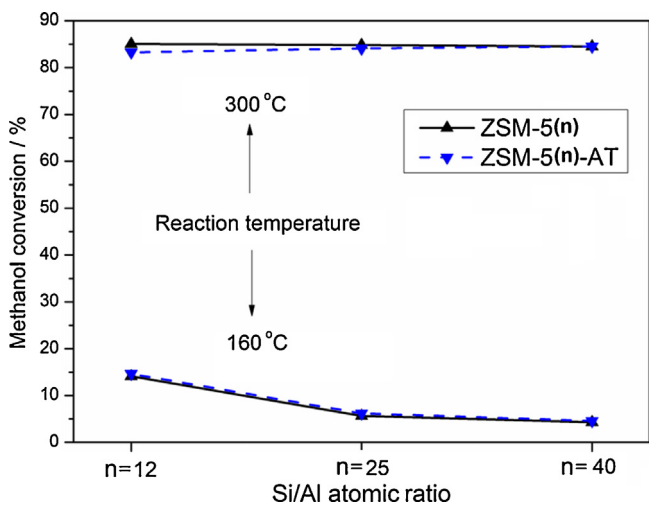


Fig. 5. Methanol conversion over fully activated parent and alkaline-treated ZSM-5 catalysts (activation temperature: 500°C ; WHSV: $13\text{ g g}^{-1}\text{ h}^{-1}$).

substantially increasing with TOS. The by-products, for instance, ethylene exhibited an opposite selectivity trend with time-on-stream of the DME selectivity. Methanol-to-hydrocarbons involves complex reaction networks in which methanol is firstly dehydrated

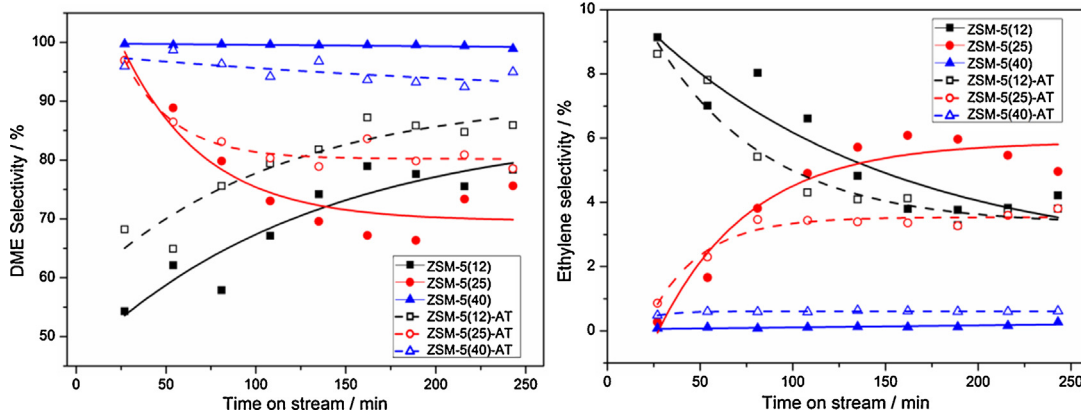


Fig. 7. DME and ethylene selectivity over fully activated parent and alkaline-treated ZSM-5 catalysts (activation temperature: 500°C ; reaction temperature: 300°C ; WHSV: $13\text{ g g}^{-1}\text{ h}^{-1}$).

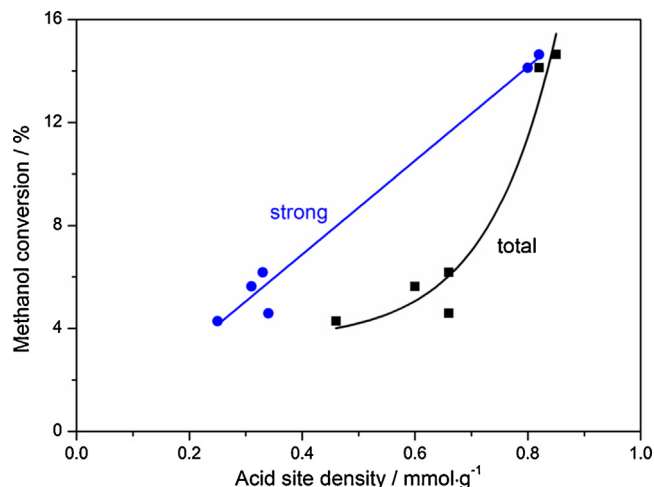


Fig. 6. Methanol conversion plotted against strong and total acid site density (activation temperature: 500°C ; reaction temperature: 160°C ; WHSV: $13\text{ g g}^{-1}\text{ h}^{-1}$; the lines are drawn to guide the eye).

to DME and then DME is converted to light olefins, aromatics and even coke. This indicates that secondary reactions occurred with the formation of hydrocarbons, which lowered DME selectivity as also described previously by Vedin and co-workers [55]. The strong acid sites are likely responsible for the occurrence of the side reactions of MTH at this temperature. In line with this, on account of the higher strong acid site density, the lower Si/Al ratio resulted in a lower DME selectivity. The previous findings reported by Schulz indicated that three stages are involved in the MTH reaction: initiation, acceleration and retardation [56]. Accordingly, it can be speculated that DME selectivity decreasing with TOS corresponded to the regime of initiation/acceleration, during which some hydrocarbons accumulated on the catalysts and promoted the MTH reaction, while DME selectivity increasing with TOS corresponded to the regime of retardation, during which coke deposited on strong acid sites and deactivated the MTH reaction.

Upon alkaline treatment, ZSM-5(12)-AT and ZSM-5(25)-AT exhibited higher DME selectivity, while ZSM-5(40)-AT exhibited somewhat lower DME selectivity. The increase of DME selectivity over ZSM-5(25)-AT is ascribed to the increase of mesoporosity, which reduced the intra-crystalline diffusion path length, lower the retention time of DME and thus decreased the probability of secondary reactions to hydrocarbons and coke [41,42]. Similar improvement on selectivity over mesoporous zeolites has also been found in other catalytic systems. For example, in the

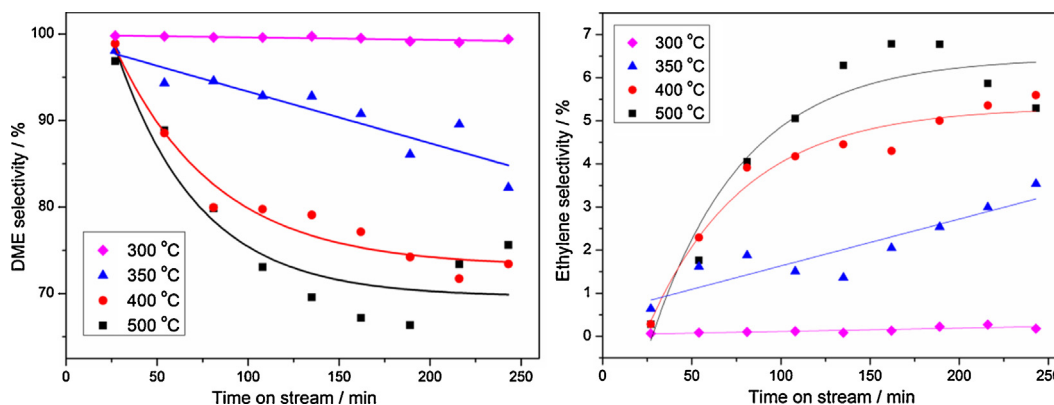


Fig. 8. Effect of activation temperature on DME and ethylene selectivity over ZSM-5(25) (reaction temperature: 300 °C; WHSV: 13 g g⁻¹ h⁻¹).

cracking of *n*-octane, Seo and co-workers found that alkali-treatment on ZSM-5 zeolite enhanced selectivity to primary cracking products due to the fast transport from the mesoporous zeolite particles [57]. Xu and co-workers found that alkaline-treated ZSM-5 exhibited improved stability in the aromatization and isomerization of 1-hexene due to the fast diffusion of desired product avoiding further conversion to coke [58]. Meanwhile, the change of the acidity by the alkaline treatment should also be taken into account. As suggested by the NH₃-TPD results in Fig. 4, the slightly lowered acid strength of the strong acid sites possibly led to the improvement of DME selectivity over ZSM-5(12)-AT which exhibited limited extra mesoporosity. The increase of strong acid site density is the proposed reason of the decrease of DME selectivity over ZSM-5(40)-AT, despite its obviously increased mesoporosity.

The effect of activation temperature on the catalytic performance at 300 °C was studied first over ZSM-5(25). As shown in Fig. 8, the activation had been carried out at 500, 400, 350 and 300 °C individually. A distinctly improved DME selectivity and decreased ethylene selectivity was achieved with decreasing activation temperature, during which methanol conversion was kept at about 84% which is close to the equilibrium conversion. The effect of the activation temperature on the physicochemical properties of ZSM-5(25) has been further characterized. ²⁷Al MAS NMR (Fig. S1) results indicate that the framework aluminum atoms were well preserved in the structure during the activation because all the parent and activated catalysts exhibited a similarly intense signal at about $\delta = 55$ ppm ascribed to the tetrahedrally coordinated framework aluminum, while only ZSM-5(25) activated at 500 °C additionally exhibited a very weak signal at about $\delta = 0$ ppm belonging to

octahedrally coordinated extra-framework aluminum possibly extracted by the activation at elevated temperature [59]. CHN elemental analysis (Table S1) showed that the *N* contents (wt%) of ZSM-5(25) activated at 300 and 500 °C were 0.5 and <0.1 respectively, which indicates that the ammonium cations were partially retained in the activated catalysts depending on the activation temperature. Accordingly, we proposed that the improvement of the DME selectivity was due to the selective blocking of strong acid sites by the retained ammonium cations, which drastically reduced the formation of hydrocarbons and coke [31]. Furthermore, the catalytic performance of the parent and alkaline-treated catalysts partially activated at 300 °C were investigated at reaction temperatures of 160 and 300 °C. Compared with the fully activated catalysts, all the partially activated catalysts as shown in Fig. 9 exhibited a decreased methanol conversion at 160 °C, but an obviously enhanced DME selectivity near 100% with methanol conversion close to 84% at 300 °C. As it has been found that methanol conversion at 160 °C is linearly dependent on strong acid site density, these results thus further prove that the partial activation is effective in selective removal of the strong acid sites that brought about the MTH side-reaction at high temperature for all these catalysts.

The catalyst stability of ZSM-5(25) and ZSM-5(25)-AT both partially activated at 300 °C has been further investigated at reaction temperature of 300 °C for prolonged time. As shown in Fig. 10, with increasing the reaction time, ZSM-5(25)-AT exhibited preservation of DME selectivity near 100% and methanol conversion around 84%, while ZSM-5(25) displayed a decline of DME selectivity and methanol conversion. CHN elemental analysis (Table S1) proved that the existence of carbon and nitrogen species in both spent

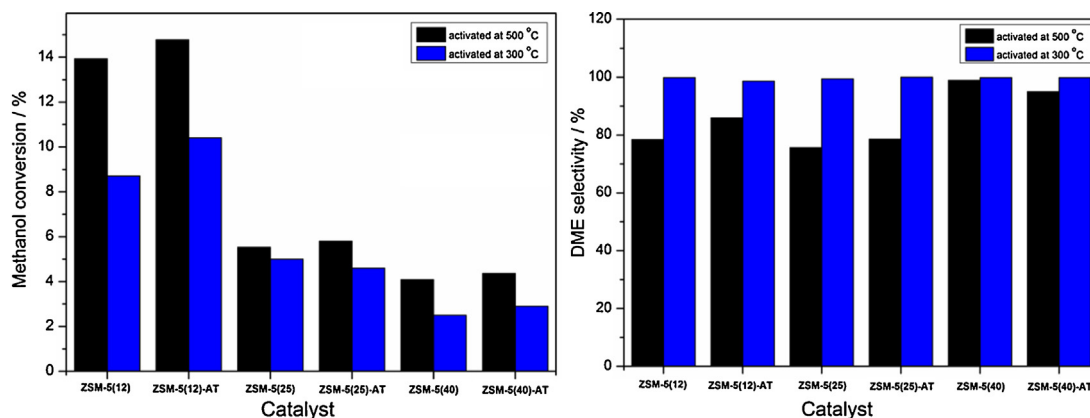


Fig. 9. Comparison of methanol conversion (left)/DME selectivity (right) over fully and partially activated ZSM-5 catalysts (activation temperature: 300 °C; reaction temperature: 160 °C (left)/300 °C (right); WHSV: 13 g g⁻¹ h⁻¹; TOS: 4 h).

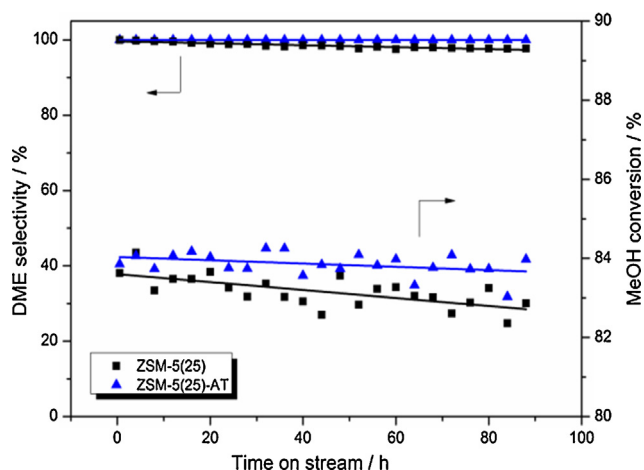


Fig. 10. Methanol dehydration performance over partially activated ZSM-5(25) and ZSM-5(25)-AT (activation temperature: 300 °C; reaction temperature: 300 °C; WHSV: 13 g g⁻¹ h⁻¹).

catalysts, which was in line with the weight loss between 300 and 800 °C calculated from the TGA curves (Fig. S2). The color of the spent ZSM-5(25)-AT showed no perceivable change, whereas that of the spent ZSM-5(25) visually turned darker, which indicate that a more severe coking caused by the MTH side reactions occurred over ZSM-5(25). It further proves that the extra mesoporosity facilitated the diffusion of the products and contributed to the alleviation of the formation of hydrocarbons and coke [41,42]. To further differentiate the catalytic activity of these two catalysts, the stability experiments were also carried out at higher WHSV. At WHSV = 28 g g⁻¹ h⁻¹ (Fig. S3), the results are fully in line with the results at WHSV = 13 g g⁻¹ h⁻¹, but still the methanol conversion was close to equilibrium. At WHSV = 112 g g⁻¹ h⁻¹ (Fig. S4), ZSM-5(25)-AT showed higher activity than ZSM-5(25) with methanol conversion remote from equilibrium. However, the two catalysts displayed similar stability, the reason of which has not been further investigated. The improved activity for the alkaline-treated sample can be explained by two factors. The first one is the increase of the acid site density due to the preferential extraction of framework silicon atoms. The second one is the improved mass transfer due to the formation of mesoporosity, which increases the accessibility to the active sites [60]. These results demonstrate that alkaline treatment leads to higher accessibility and acidity that showed up as higher stability at lower WHSV and higher activity at very high WHSV. At the same time, the enhanced catalytic performance over partially activated ZSM-5(25)-AT also manifests that combining partial activation and alkaline treatment is an effective method to prepare ZSM-5 catalysts with both moderated acidity and improved diffusion capability for the MTD reaction.

5. Conclusion

The effects of alkaline treatment and activation temperature over a series of commercial NH₄⁺-form ZSM-5 catalysts with Si/Al ratio of 12, 25 and 40 has been investigated for the methanol dehydration to DME reaction. When fully activated at 500 °C, all the parent and alkaline-treated catalysts exhibited 100% DME selectivity and stable catalytic activity at 160 °C, but decline of DME selectivity and methanol conversion at 300 °C as a result of the formation of hydrocarbons and coke. The parent catalysts with lower Si/Al ratio on account of their higher strong acid site density showed a lower DME selectivity at 300 °C. Compared with the parent materials, the alkaline-treated catalysts showed altered DME selectivity as a result of the change of acidity and texture properties. The

improvement or deterioration over ZSM-5(12)-AT and ZSM-5(40)-AT are tentatively ascribed to the decrease or increase of strong acid sites that brought about the MTH reaction. The improved selectivity to DME over ZSM-5(25)-AT indicates that the formation of extra mesoporosity enhanced diffusion capability and decreased the probability of secondary reactions of DME to hydrocarbons and coke. Decreasing the activation temperature of the NH₄⁺-ZSM-5 precursors significantly improved DME selectivity for all the parent and alkaline-treated ZSM-5 because the remaining ammonium cations in the structure selectively blocked the strong acid sites and avoided the occurrence of side-reactions. Applying partial activation at 300 °C, ZSM-5(25)-AT compared with ZSM-5(25) showed an improved stability with almost 100% DME selectivity and nearly 84% methanol conversion for 4 days of reaction at reaction temperature of 300 °C and WHSV of 13 g g⁻¹ h⁻¹. ZSM-5 modified by combining alkaline treatment and partial activation could be promising as part of an integrated catalyst for producing DME directly from synthesis gas due to the moderated acidity, enhanced diffusion capability as well as the simple and effective preparation method. The tailoring of both acidity and accessibility of zeolites using the approach described in this paper could be of wider use to the adsorption and catalysis community.

Acknowledgments

The authors thank BP International Limited for financial support and Dr. David Apperley at Durham University for NMR characterization.

Appendix A. Supplementary data

Supplementary data associated with this article can be found, in the online version, at <http://dx.doi.org/10.1016/j.apcata.2014.12.027>.

References

- [1] T.A. Semelsberger, R.L. Borup, H.L. Greene, *J. Power Sources* 156 (2006) 497–511.
- [2] C. Arcoumanis, C. Bae, R. Crookes, E. Kinoshita, *Fuel* 87 (2008) 1014–1030.
- [3] T.H. Fleisch, A. Basu, R.A. Sills, *J. Nat. Gas Sci. Eng.* 9 (2012) 94–107.
- [4] Z. Azizi, M. Rezaei-Manesh, T. Tohidian, M.R. Rahimpour, *Chem. Eng. Process.* 82 (2014) 150–172.
- [5] M.T. Xu, J.H. Lunsford, D.W. Goodman, A. Bhattacharyya, *Appl. Catal. A* 149 (1997) 289–301.
- [6] Q.J. Ge, Y.M. Huang, F.Y. Qiu, S.B. Li, *Appl. Catal. A* 167 (1998) 23–30.
- [7] R. Montesano, A. Narvaez, D. Chadwick, *Appl. Catal. A* 482 (2014) 69–77.
- [8] K.W. Jun, H.S. Lee, H.S. Roh, S.E. Park, *Bull. Korean Chem. Soc.* 23 (2002) 803–806.
- [9] F. Raouf, M. Taghizadeh, A. Eliassi, F. Yaripour, *Fuel* 87 (2008) 2967–2971.
- [10] Y. Fu, T. Hong, J. Chen, A. Auroux, J. Shen, *Thermochim. Acta* 434 (2005) 22–26.
- [11] S.S. Akarmazyan, P. Panagiotopoulou, A. Kambolis, C. Papadopoulou, D.I. Kondarides, *Appl. Catal. B* 145 (2014) 136–148.
- [12] S.Y. Hosseini, M.R.K. Nikou, *J. Ind. Eng. Chem.* 20 (2014) 4421–4428.
- [13] M. Ghavipour, R.M. Behbahani, *J. Ind. Eng. Chem.* 20 (2014) 1942–1951.
- [14] A.S. Rocha, A.M. da, S. Forrester, E.R. Lachter, E.F. Sousa-Aguiar, A.C. Faro, *Catal. Today* 192 (2012) 104–111.
- [15] V. Vishwanathan, H.S. Roh, J.W. Kim, K.W. Jun, *Catal. Lett.* 96 (2004) 23–28.
- [16] A.E.-A.A. Said, M.M. Abd El-Wahab, M.A. El-Aal, *J. Mol. Catal. A: Chem.* 394 (2014) 40–47.
- [17] B. Sabour, M.H. Peyrovi, T. Hamoule, M. Rashidzadeh, *J. Ind. Eng. Chem.* 20 (2014) 222–227.
- [18] Y. Sang, H. Li, M. Zhu, K. Ma, Q. Jiao, Q. Wu, *J. Porous Mater.* 20 (2013) 1509–1518.
- [19] P.S. Sai Prasad, J.W. Bae, S.-H. Kang, Y.-J. Lee, K.-W. Jun, *Fuel Process. Technol.* 89 (2008) 1281–1286.
- [20] J. Bandiera, C. Naccache, *Appl. Catal.* 69 (1991) 139–148.
- [21] D. Mao, J. Xia, Q. Chen, G. Lu, *Catal. Commun.* 10 (2009) 620–624.
- [22] P.G. Moses, J.K. Nørskov, *ACS Catal.* 3 (2013) 735–745.
- [23] D. Jin, B. Zhu, Z. Hou, J. Fei, H. Lou, X. Zheng, *Fuel* 86 (2007) 2707–2713.
- [24] L. Vanoye, A. Favre-Régouillon, P. Munno, J.F. Rodríguez, S. Dupuy, S. Pallier, I. Pitault, C. De Bellefon, *Catal. Today* 215 (2013) 239–242.
- [25] G. Laugel, X. Nitsch, F. Ocampo, B. Louis, *Appl. Catal. A* 402 (2011) 139–145.
- [26] J.W. Bae, S.-H. Kang, Y.-J. Lee, K.-W. Jun, *Appl. Catal. B* 90 (2009) 426–435.
- [27] M. Migliori, A. Aloise, E. Catizzone, G. Giordano, *Ind. Eng. Chem. Res.* 53 (2014) 14885–14891.

- [28] W. Dai, W. Kong, G. Wu, N. Li, L. Li, N. Guan, *Catal. Commun.* 12 (2011) 535–538.
- [29] K. Lertjiamratn, P. Prasertthadam, M. Arai, J. Panpranot, *Appl. Catal. A* 378 (2010) 119–123.
- [30] G. Pop, G. Bozga, R. Ganea, N. Natu, *Ind. Eng. Chem. Res.* 48 (2009) 7065–7071.
- [31] J. Topp-Jorgensen, *US Patent* 4 536 485 (1985).
- [32] J.F. Haw, W.G. Song, D.M. Marcus, J.B. Nicholas, *Acc. Chem. Res.* 36 (2003) 317–326.
- [33] U. Olsbye, S. Svelle, M. Bjørgen, P. Beato, T.V. Janssens, F. Joensen, S. Bordiga, K.P. Lillerud, *Angew. Chem. Int. Ed.* 51 (2012) 5810–5831.
- [34] A. García-Trencó, S. Valencia, A. Martínez, *Appl. Catal. A* 468 (2013) 102–111.
- [35] B. Yilmaz, U. Müller, *Top. Catal.* 52 (2009) 888–895.
- [36] F. Mohammadparast, R. Halladj, S. Askari, *Chem. Eng. Commun.* 202 (2015) 542–556.
- [37] N. Khandan, M. Kazemeini, M. Aghaziarati, *Appl. Catal. A* 349 (2008) 6–12.
- [38] V. Vishwanathan, K.-W. Jun, J.-W. Kim, H.-S. Roh, *Appl. Catal. A* 276 (2004) 251–255.
- [39] D. Mao, W. Yang, J. Xia, B. Zhang, Q. Song, Q. Chen, *J. Catal.* 230 (2005) 140–149.
- [40] S. Hassanpour, F. Yaripour, M. Taghizadeh, *Fuel Process. Technol.* 91 (2010) 1212–1221.
- [41] A.A. Rownaghi, F. Rezaei, M. Stante, J. Hedlund, *Appl. Catal. B* 119–120 (2012) 56–61.
- [42] Q. Tang, H. Xu, Y. Zheng, J. Wang, H. Li, J. Zhang, *Appl. Catal. A* 413–414 (2012) 36–42.
- [43] H. Li, S. He, K. Ma, Q. Wu, Q. Jiao, K. Sun, *Appl. Catal. A* 450 (2013) 152–159.
- [44] Q. Yang, H. Zhang, M. Kong, X. Bao, J. Fei, X. Zheng, *Chin. J. Catal.* 34 (2013) 1576–1582.
- [45] S. van Donk, A.H. Janssen, J.H. Bitter, K.P. de Jong, *Catal. Rev. Sci. Eng.* 45 (2003) 297–319.
- [46] D. Verboekend, J. Pérez-Ramírez, *Catal. Sci. Technol.* 1 (2011) 879–890.
- [47] R. Chal, C. Gérardin, M. Bulut, S. van Donk, *ChemCatChem* 3 (2011) 67–81.
- [48] M. Bjørgen, F. Joensen, M. Spangsbørg Holm, U. Olsbye, K.P. Lillerud, S. Svelle, *Appl. Catal. A* 345 (2008) 43–50.
- [49] J. Kim, M. Choi, R. Ryoo, *J. Catal.* 269 (2010) 219–228.
- [50] B.C. Lippens, J.H. de Boer, *J. Catal.* 4 (1965) 319–323.
- [51] E.P. Barrett, L.G. Joyner, P.P. Halenda, *J. Am. Chem. Soc.* 73 (1951) 373–380.
- [52] J.C. Groen, J.A. Moulijn, J. Pérez-Ramírez, *J. Mater. Chem.* 16 (2006) 2121–2131.
- [53] M. Ogura, S.Y. Shinomiya, J. Tateno, Y. Nara, M. Nomura, E. Kikuchi, M. Matsukata, *Appl. Catal. A* 219 (2001) 33–43.
- [54] B.T. Diep, M.S. Wainwright, *J. Chem. Eng. Data* 32 (1987) 330–333.
- [55] P. Dejaifve, J.C. Vedrine, V. Bolis, E.G. Derouane, *J. Catal.* 63 (1980) 331–345.
- [56] H. Schulz, *Catal. Today* 154 (2010) 183–194.
- [57] J.S. Jung, J.W. Park, G. Seo, *Appl. Catal. A* 288 (2005) 149–157.
- [58] Y. Li, S. Liu, Z. Zhang, S. Xie, X. Zhu, L. Xu, *Appl. Catal. A* 338 (2008) 100–113.
- [59] W. Zhang, X. Han, X. Liu, X. Bao, *Microporous Mesoporous Mater.* 50 (2001) 13–23.
- [60] A.N.C. van laak, R.W. Gosseink, S.L. Sagala, J.D. Meeldijk, P.E. de Jongh, K.P. de Jong, *Appl. Catal. A* 382 (2010) 65–72.